PHILOSOPHICAL TRANSACTIONS OF THE ROYAL SOCIETY A MATHEMATICAL, PHYSICAL & ENGINEERING SCIENCES

Analysis of atrial fibrillation: from electrocardiogram signal processing to clinical management

Leif Sörnmo, Martin Stridh, Daniela Husser, Andreas Bollmann and S. Bertil Olsson

Phil. Trans. R. Soc. A 2009 **367**, 235-253
doi: 10.1098/rsta.2008.0162

PHILOSOPHICAL TRANSACTIONS OF THE ROYAL SOCIETY A

Phil. Trans. R. Soc. A (2009) **367**, 235–253
doi:10.1098/rsta.2008.0162
Published online 24 October 2008

Review

Analysis of atrial fibrillation: from electrocardiogram signal processing to clinical management

By Leif Sörnmo[1,2,*], Martin Stridh[1,2], Daniela Husser[3], Andreas Bollmann[3] and S. Bertil Olsson[2,4]

[1]*Department of Electrical and Information Technology, and*
[2]*Center of Integrative Electrocardiology, Lund University, 221 00 Lund, Sweden*
[3]*Department of Electrophysiology, Heart Center Leipzig, 04289 Leipzig, Germany*
[4]*Department of Cardiology, Lund University, 221 85 Lund, Sweden*

The analysis of atrial fibrillation in non-invasive ECG recordings has received considerable attention in recent years, spurring the development of signal processing techniques for more advanced characterization of the atrial waveforms than previously available. The present paper gives an overview of different approaches to the extraction of atrial activity in the ECG and to the characterization of the resulting atrial signal with respect to its spectral properties. So far, the repetition rate of the atrial waves is the most studied parameter and its significance in clinical management is briefly considered, including the identification of pathomechanisms and prediction of therapy efficacy.

Keywords: atrial fibrillation; QRST cancellation; atrial frequency/rate; time–frequency analysis; clinical atrial fibrillation management

1. Introduction

Atrial fibrillation (AF) is the most commonly encountered arrhythmia in clinical practice and continues to receive considerable research interest. In recent years, various therapies have been introduced into clinical practice such as new antiarrhythmic drugs and catheter ablation techniques. However, current AF management guidelines provide no treatment recommendations that take the various mechanisms and patterns of AF into account and therefore tests are currently being developed that quantify AF and guide its management. Although the standard 12-lead electrocardiogram (ECG) is recorded in virtually every patient with AF, it is only recently that information carried by the f-waves has been explored in some detail (Bollmann *et al.* 2006).

* Author and address for correspondence: Department of Electrical and Information Technology, Lund University, 22100 Lund, Sweden (leif.sornmo@eit.lth.se).

One contribution of 13 to a Theme Issue ‘Signal processing in vital rhythms and signs’.

The estimation of the atrial fibrillatory frequency, i.e. the repetition rate of the atrial waves, has so far been the main signal processing challenge to address. This is due to the fact that the atrial activity must be extracted by some technique in the presence of the much larger ventricular activity. The extraction requires nonlinear signal processing because atrial and ventricular activity overlap spectrally and therefore cannot be separated by linear filtering. The design of extraction algorithms is based on different physiological observations such as atrial and ventricular activity being uncoupled during AF or atrial and ventricular activity originating from independent electrical sources. Clinically, it has been shown that AF is more likely to terminate spontaneously and respond better to antiarrhythmic drugs or cardioversion at low fibrillatory rates, whereas AF is more often persistent and refractory to therapy at high rates (Bollmann *et al.* 2006).

The availability of an atrial signal makes it possible to perform power spectral analysis for the purpose of locating the dominant AF frequency. From an electrophysiological viewpoint, however, there are reasons to believe that the fibrillatory waves have time-dependent properties since they reflect complex patterns of electrical activation wavefronts. Therefore, when more detailed information is needed, time–frequency analysis can be employed in order to track variations in frequency (Mainardi *et al.* 2008).

The present paper gives an overview of signal processing techniques developed for the analysis of AF in ECG recordings. In particular, different techniques for atrial activity extraction (§2) and time–frequency analysis (§3) are described, followed by an overview of clinical applications where these techniques are crucial for characterization of AF (§4).

2. Atrial activity extraction

The average beat subtraction (ABS) method was initially developed to facilitate identification of P-waves during ventricular tachycardia (Slocum *et al.* 1985). Later, this method was applied to AF analysis for the purpose of extracting the f-waves that are contiguous in nature (Slocum *et al.* 1992; Bollmann *et al.* 1998; Holm *et al.* 1998). In both applications, the ECG signal was processed on a single-lead basis so that an average beat, representative of the ventricular cycle, was subtracted from each individual heartbeat. The resulting atrial (residual) signal would, ideally, contain the fibrillatory waveforms subjected to further analysis.

The average beat is computed from an ensemble of time-aligned sinus beats contained in the segment to be processed, thus assuming that the beat morphologies have been clustered. Prior to subtraction, it is crucial to ensure that the average beat and each QRST complex are well-aligned in time to each other. If not, the resulting atrial signal will contain QRST residuals, and subsequent processing is rendered much more difficult. Therefore, temporal alignment is required in any method that involves subtraction of the average beat. The alignment problem is defined by

$$\epsilon^2_{\min} = \min_{\tau} \|\boldsymbol{x} - \boldsymbol{J}_\tau \bar{\boldsymbol{x}}\|^2, \tag{2.1}$$

where ϵ^2 denotes quadratic error defined by the vector norm and the vector $\boldsymbol{x}$ denotes N samples of the observed signal $x(n)$,

$$\boldsymbol{x} = [\, x(0) \quad x(1) \quad \ldots \quad x(N-1) \,]^{\mathrm{T}}. \tag{2.2}$$

The average beat $\bar{\boldsymbol{x}}$ contains 2Δ additional samples so as to allow for temporal alignment of $\boldsymbol{x}$ relative $\bar{\boldsymbol{x}}$ using the shift matrix $\boldsymbol{J}_\tau$,

$$\boldsymbol{J}_\tau = [\, \boldsymbol{0}_{N\times(\Delta+\tau)} \quad \boldsymbol{I}_{N\times N} \quad \boldsymbol{0}_{N\times(\Delta-\tau)} \,], \tag{2.3}$$

where τ denotes an integer time shift. The two matrices $\boldsymbol{0}$ and $\boldsymbol{I}$ denote the zero and identity matrix, respectively. The maximal alignment error that can be corrected with this formulation is $\pm\Delta$. The minimization is performed as a grid search over all admissible values of τ, thus determining the N samples of $\bar{\boldsymbol{x}}$ which best fit $\boldsymbol{x}$.

(*a*) *Spatio-temporal QRST cancellation*

ABS relies on the assumption that an average beat represents each individual beat accurately. However, the QRST morphology is often subject to minor changes due to variations in the orientation of the heart's electrical axis. These variations are primarily due to respiratory activity and influence the precordial leads quite considerably. Owing to the single-lead nature of ABS, such axis variations sometimes cause considerable QRST-related residuals.

The spatio-temporal method (Stridh & Sörnmo 2001) assumes that a multi-lead ECG is available, and, consequently, the data vector in (2.2) is replaced by a data matrix $\boldsymbol{X}$ with N samples from L leads,

$$\boldsymbol{X} = [\, \boldsymbol{x}_1 \quad \boldsymbol{x}_2 \quad \ldots \quad \boldsymbol{x}_L \,]. \tag{2.4}$$

Since atrial activity is assumed to be uncoupled to ventricular activity during AF, each observed beat $\boldsymbol{X}$ can be modelled as a sum of atrial activity $\boldsymbol{X}_{\mathrm{A}}$, ventricular activity $\boldsymbol{X}_{\mathrm{V}}$ and additive noise $\boldsymbol{W}'$,

$$\boldsymbol{X} = \boldsymbol{X}_{\mathrm{A}} + \boldsymbol{X}_{\mathrm{V}} + \boldsymbol{W}'. \tag{2.5}$$

The ventricular activity is modelled by

$$\boldsymbol{X}_V = \boldsymbol{J}_\tau \bar{\boldsymbol{X}} \boldsymbol{S}, \tag{2.6}$$

where $\boldsymbol{S}$ is a spatial alignment matrix ($L\times L$) that allows transferring of information between leads to compensate for variations in the electrical axis, and scaling to compensate for variations in tissue conductivity and heart position. The matrix $\boldsymbol{S}$ is assumed to be the product of a diagonal amplitude scaling matrix $\boldsymbol{D}$ and a rotation matrix $\boldsymbol{Q}$, i.e.

$$\boldsymbol{S} = \boldsymbol{D}\boldsymbol{Q}, \tag{2.7}$$

where the diagonal elements d_l of $\boldsymbol{D}$ are assumed to be positive-valued.

Ultimately, the aim is to estimate the parameters $\boldsymbol{D}$, $\boldsymbol{Q}$ and τ from the observed signal $\boldsymbol{X}$, and then to subtract the resulting estimate of $\boldsymbol{X}_{\mathrm{V}}$ from $\boldsymbol{X}$. However, combining (2.5) and (2.6) such that

$$\boldsymbol{X} - \boldsymbol{J}_\tau \bar{\boldsymbol{X}} \boldsymbol{S} = \boldsymbol{W}' + \boldsymbol{X}_{\mathrm{A}}, \tag{2.8}$$

it is immediately clear that not only $\boldsymbol{W}'$ limits how well $\boldsymbol{J}_\tau\bar{\boldsymbol{X}}\boldsymbol{S}$ will fit $\boldsymbol{X}$, but so also does $\boldsymbol{X}_\mathrm{A}$. In order to handle this problem, an intermediate estimate can be introduced, $\tilde{\boldsymbol{X}}_\mathrm{A}$, to be subtracted from both sides of (2.8) prior to parameter estimation

$$\boldsymbol{Y}-\boldsymbol{J}_\tau\bar{\boldsymbol{X}}\boldsymbol{S}=\boldsymbol{W}'+\boldsymbol{X}_\mathrm{A}-\tilde{\boldsymbol{X}}_\mathrm{A}, \tag{2.9}$$

where $\boldsymbol{Y}=\boldsymbol{X}-\tilde{\boldsymbol{X}}_\mathrm{A}$. The process of subtracting $\tilde{\boldsymbol{X}}_\mathrm{A}$ in (2.9) is based on the availability of a TQ-based AF signal that, for example, can be computed from TQ intervals containing f-waves free of ventricular activity. Interpolation between successive TQ intervals is used to fill in the intermediate QT interval with atrial activity (Stridh & Sörnmo 2001; Castells *et al.* 2005*b*).

The parameters $\boldsymbol{D}$, $\boldsymbol{Q}$ and τ are estimated by solving the minimization problem,

$$\epsilon^2_{\min}=\min_{\boldsymbol{D},\boldsymbol{Q},\tau}\|\boldsymbol{Y}-\boldsymbol{J}_\tau\bar{\boldsymbol{X}}\boldsymbol{D}\boldsymbol{Q}\|^2_\mathrm{F}, \tag{2.10}$$

where the quadratic error is defined by the Frobenius norm $\|\boldsymbol{A}\|^2_\mathrm{F}=\mathrm{tr}(\boldsymbol{A}\boldsymbol{A}^\mathrm{T})$.

Minimization with respect to $\boldsymbol{Q}$ and $\boldsymbol{D}$ requires an alternating, iterative approach in which the error in (2.10) is minimized with respect to $\boldsymbol{Q}$, assuming that $\boldsymbol{D}$ is known. The minimization involves the singular value decomposition (SVD) with which an arbitrary matrix $\boldsymbol{T}$ is decomposed into two orthonormal matrices, $\boldsymbol{U}$ and $\boldsymbol{V}$, and a diagonal matrix $\boldsymbol{\Sigma}$ that contains the singular values σ_l,

$$\boldsymbol{T}=\boldsymbol{U}\boldsymbol{\Sigma}\boldsymbol{V}^\mathrm{T}. \tag{2.11}$$

By setting $\boldsymbol{T}=\boldsymbol{D}^\mathrm{T}\bar{\boldsymbol{X}}^\mathrm{T}\boldsymbol{J}_\tau^\mathrm{T}\boldsymbol{Y}$ and performing the SVD, the error is minimized for

$$\hat{\boldsymbol{Q}}=\boldsymbol{U}\boldsymbol{V}^\mathrm{T}. \tag{2.12}$$

Next, with an estimate of $\boldsymbol{Q}$ available, the optimal diagonal entries of $\boldsymbol{D}$ can be estimated by (Stridh & Sörnmo 2001)

$$\hat{d}_l=\left([\boldsymbol{J}_\tau\bar{\boldsymbol{X}}]_l^\mathrm{T}[\boldsymbol{J}_\tau\bar{\boldsymbol{X}}]_l\right)^{-1}([\boldsymbol{J}_\tau\bar{\boldsymbol{X}}]_l^\mathrm{T}[\boldsymbol{Z}\boldsymbol{Q}^{-1}]_l),\quad l=1,2,\ldots,L, \tag{2.13}$$

where $[\cdot]_l$ denotes the l-th column of the matrix. An improved estimate of $\boldsymbol{Q}$ can then be obtained from (2.12) using the estimate of $\boldsymbol{D}$, and so on. Finally, minimization with respect to τ is solved through a grid search of τ in the interval $[-\Delta,\Delta]$.

Figure 1 illustrates the performance of spatio-temporal cancellation and ABS, showing that the QRST-related residuals are much smaller for the former method.

(*b*) *Separate processing of QRS and T*

The idea to process the QRS complex and T-wave with separate averages was initially suggested in Waktare *et al.* (1998), but later refined and evaluated in Lemay *et al.* (2007). An important motivation to pursue separate processing is that the repolarization waveform changes in relation to heart rate whereas the depolarization waveform remains unchanged. In this approach, the average beat $\bar{\boldsymbol{X}}$ is decomposed into two submatrices that contain the averaged samples of the QRS and JQ intervals, respectively; the JQ interval starts at the J point and ends at Q onset of the subsequent beat. In doing so, the two intervals can be processed differently with respect to which beat intervals to include for beat averaging, and how to fit the average beat to the observed signal. A disadvantage with separate processing of QRS and T is that discontinuities may occur at the

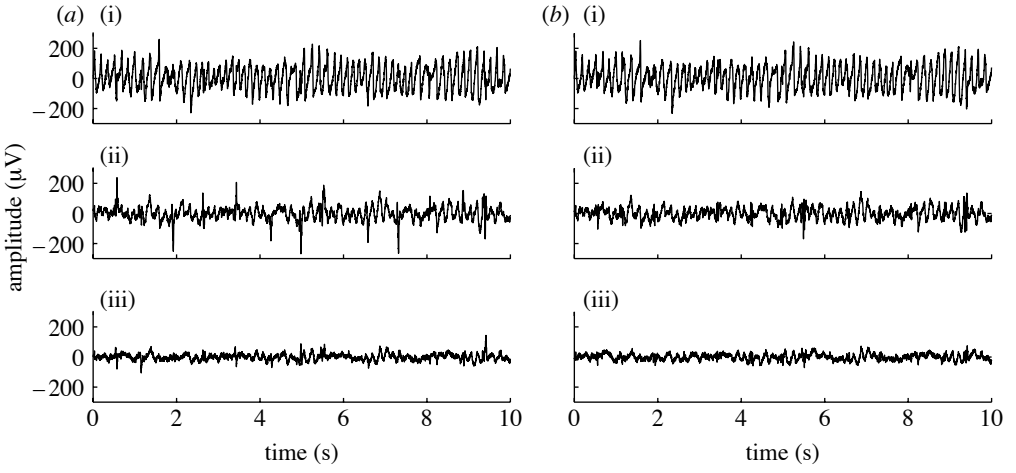

Figure 1. Extracted atrial signals in leads (i) V1, (ii) V2 and (iii) V3 using (*a*) ABS and (*b*) spatio-temporal QRST cancellation.

boundaries. This problem can be mitigated with low-pass filtering, for example, using a zero-phase, fifth-order Butterworth filter with cut-off frequency at 50 Hz (Lemay *et al.* 2007).

(*c*) *Single beat cancellation*

The single beat cancellation method processes one heartbeat at a time, and does not, in contrast to the previous methods of this paper, make use of information acquired from the beat averaging process (Lemay *et al.* 2007). The main idea is to estimate the dominant T-wave morphology in each individual beat, using all available leads, and subtract it from the original ECG. The atrial activity within the QRS interval is estimated from interpolation of the atrial activity contained in the two enclosing JQ intervals, and, thus, no attempt is made to retrieve the atrial information being concealed within the QRS interval.

It has been observed that T-wave morphology in different ECG leads is quite similar—an observation that gave rise to the concept of 'the dominant T-wave', found useful for representing individual T-waves (van Oosterom 2003). The dominant T-wave may be estimated from the $N\times L$ data matrix $\boldsymbol{X}$, containing the N samples of the JQ interval from the L-lead ECG, as the most significant eigenvector, i.e. computing the SVD of $\boldsymbol{X}$ and choosing that eigenvector (i.e. column) of $\boldsymbol{U}$ which corresponds to the largest singular value.

In order to provide flexible modelling of each individual T-wave, the dominant T-wave is defined as a linear combination of the most significant eigenvector and its time derivatives. However, since the eigenvector contains noise that may influence the derivatives quite considerably, it is necessary to fit a smooth analytical function to the eigenvector and then compute the time derivatives from the fitted function. Nonlinear optimization is employed to find the values that best fit the eigenvector.

Next, each ECG lead is modelled as a linear combination of the fitted function and two of its time derivatives. The coefficients are obtained jointly for all leads using least-squares estimation. Within the JQ interval, an atrial signal is then produced by subtracting the estimate of the dominant T-wave from the ECG.

The atrial activity during the QRS interval is not extracted from the ECG signal, but results from interpolation of the atrial signals of the JQ intervals that enclose the QRS interval to be processed (Lemay *et al.* 2007). Employing sinusoidal interpolation, the coefficients that define the linear combination of sines and cosines at different frequencies are determined using least-squares estimation. Finally, the atrial signal is obtained by concatenating the enclosing JQ intervals with the sinusoidal signal obtained from interpolation. Since the concatenated signal may contain jumps at the interval boundaries, low-pass filtering is performed as the final step.

(*d*) *Principal component analysis*

Principal components analysis (PCA) performs an orthogonal linear transformation of the data such that the resulting principal components (PCs) contain maximal information, measured by variance, and minimal redundancy, measured by correlation (Joliffe 2002). The first PC is a linear combination of the data that maximize the joint variance in the least-squares sense. The second PC holds the second largest variance, constrained to be uncorrelated with the first PC, and so on. It is assumed that the signal vector $\boldsymbol{x}$ is a zero-mean random process, characterized by the correlation matrix $\boldsymbol{R}_x = E[\boldsymbol{x}\boldsymbol{x}^{\mathrm{T}}]$. The PCs $\boldsymbol{w} = [\, w_1 \quad w_2 \quad \ldots \quad w_N \,]^{\mathrm{T}}$ result from an orthogonal linear transformation $\boldsymbol{\Psi} = [\, \psi_1 \quad \psi_2 \quad \ldots \quad \psi_N \,]$ of $\boldsymbol{x}$,

$$\boldsymbol{w} = \boldsymbol{\Psi}^{\mathrm{T}} \boldsymbol{x}, \tag{2.14}$$

which rotates $\boldsymbol{x}$ so that the elements of $\boldsymbol{w}$ become mutually uncorrelated. In order to obtain the set of N PCs, the eigenvector equation for $\boldsymbol{R}_x$ has to be solved. The eigenvector ψ_1, corresponding to the largest eigenvalue, is associated with the largest variance of the signal, and so on. Since $\boldsymbol{R}_x$ is not known in practice, it is replaced by the sample correlation matrix $\hat{\boldsymbol{R}}_x$ estimated from the data ensemble.

PCA-based extraction of atrial activity can be applied to single-lead ECGs, becoming a technique for finding data-dependent functions for QRST cancellation, or multi-lead ECGs, becoming a technique for blind source separation. Since the two techniques process the ECG signal in different ways, relying on different definitions of the data matrix $\boldsymbol{X}$, the techniques are described separately.

In single-lead PCA, the ventricular activity to be cancelled is characterized in terms of intra-beat correlation, and, consequently, temporal properties are exploited rather than spatial ones (Castells *et al.* 2005*a*, 2007). The data matrix contains an ensemble of M single-lead beats with N samples, represented by the $N \times M$ matrix

$$\boldsymbol{X} = [\, \boldsymbol{x}_1 \quad \boldsymbol{x}_2 \quad \ldots \quad \boldsymbol{x}_M \,]. \tag{2.15}$$

It should be noted that this definition of $\boldsymbol{X}$ differs from the one introduced in (2.4) which contains several leads of one single beat. The number of beats M should be chosen large enough to produce a useful estimate of $\boldsymbol{R}_x$. While $\boldsymbol{X}$ may be allowed to contain beats of different morphologies, it may be desirable to select beats with similar morphology as this choice implies that a smaller value of M is required. The N samples from each beat are selected with reference to a fiducial point such that the entire QRST complex is included in the segment, possibly overlapping with adjacent beats. The $N \times N$ sample correlation matrix is obtained by

$$\hat{\boldsymbol{R}}_x = \frac{1}{M}\boldsymbol{X}\boldsymbol{X}^{\mathrm{T}}. \tag{2.16}$$

Applying PCA to the ensemble of beats, the associated pattern of PCs reflects the degree of morphologic beat-to-beat variability: when the largest eigenvalue is much larger than the other ones, the ensemble of beats exhibits low morphologic variability, whereas a gradual fall-off indicates large variability. The eigenvector corresponding to the largest eigenvalue is related to the dominant QRST morphology since the ventricular activity exhibits the largest variance in the ECG. The next few eigenvectors correspond to QRST dynamics; in the case of a very stable morphology, these components are missing. Next, a few eigenvectors relate to atrial activity, whereas the remaining eigenvectors relate to various noise sources.

Since PCA projects each beat on the 'ventricular subspace', a QRST waveform can be estimated and removed by subtracting a linear combination of the 'ventricular' eigenvectors. Alternatively, atrial activity can be extracted from each beat by considering the projection on the 'atrial subspace'. Needless to say, the performance of PCA is critically dependent on the algorithm being employed for subspace identification. This aspect is mentioned in Castells *et al.* (2005*a*), although details of the algorithm employed for identification are not given.

Another approach to the extraction of atrial activity is to explore the redundant information of multi-lead ECGs (Langley *et al.* 2000; Raine *et al.* 2004). By applying PCA, it is possible to decompose the multi-lead ECG so that the most representative component is the one which corresponds to ventricular activity, whereas the next few components correspond to variability in ventricular activity (see above). The next PCs usually contain atrial activity.

In multi-lead PCA, the definition of the data matrix is identical to that used for spatio-temporal QRST cancellation, i.e.

$$\boldsymbol{X} = [\,\boldsymbol{x}_1 \quad \boldsymbol{x}_2 \quad \ldots \quad \boldsymbol{x}_L\,], \tag{2.17}$$

where L denotes the number of leads which, in most studies, equals eight because the standard 12-lead ECG is analysed. Rather than characterizing intra-beat correlation as in (2.16), multi-lead PCA exploits inter-lead correlation by computing

$$\hat{\boldsymbol{R}}_x = \frac{1}{N}\boldsymbol{X}^{\mathrm{T}}\boldsymbol{X}. \tag{2.18}$$

As before, the eigenvectors $\boldsymbol{\Psi}$ that result from diagonalization of $\hat{\boldsymbol{R}}_x$ define the orthogonal linear transformation used to compute the PCs. In this case, the PCs are computed for each sample n by

$$\boldsymbol{w}(n) = \boldsymbol{\Psi}^{\mathrm{T}}\boldsymbol{x}(n), \tag{2.19}$$

where $\boldsymbol{x}(n) = [\,x_1(n) \quad x_2(n) \quad \ldots \quad x_L(n)\,]^{\mathrm{T}}$. Figure 2 presents an example where PCA is applied to an ECG with AF. The atrial activity can be identified as the fourth PC, whereas the three first components contain ventricular activity and some noise. The higher order components contain noise that largely is of muscular origin. Similar to single-lead PCA, algorithms for identification of the atrial subspace remain to be devised.

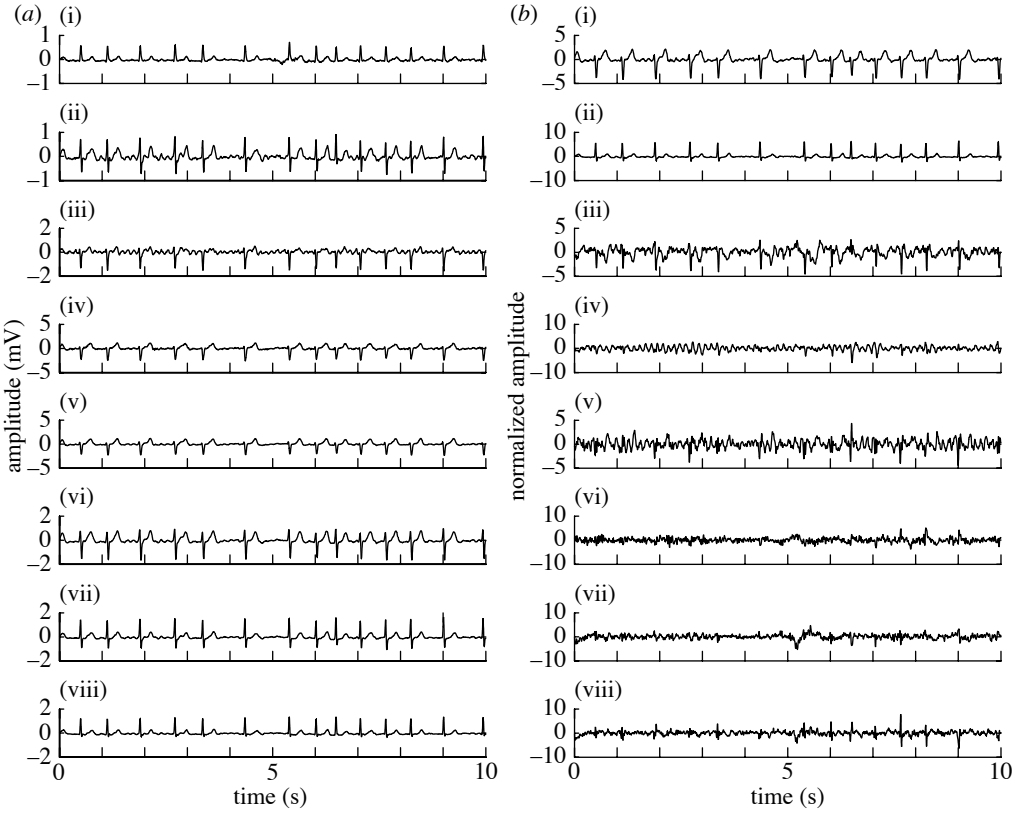

Figure 2. Example of atrial signal extraction during AF using a multi-lead PCA approach. (*a*) The original eight-lead ECG (i) I, (ii) II, (iii–viii) V1–V6 and (*b*) associated PCs, i.e. $\boldsymbol{w}(n)$ (i–viii) PC1–PC8.

(*e*) *Independent component analysis*

Another approach to atrial activity extraction is to assume that the observed signal is a mixture of different signal sources of atrial, ventricular and extracardiac origin. Although blind separation of signal sources can be accomplished by the above-mentioned second-order PCA approach, it is often desirable to develop a technique that exploits higher order statistics in order to achieve better performance when the signal is not Gaussian. The following linear model is the starting point for such separation:

$$\boldsymbol{x}(n) = \boldsymbol{A}\boldsymbol{s}(n), \tag{2.20}$$

where $\boldsymbol{A}$ denotes an $L \times L$ instantaneous mixing matrix; $\boldsymbol{s}(n)$ is a vector with L different source signals at time n; and $\boldsymbol{x}(n)$ is another vector with the observations of L different 'sensor' signals obtained from the ECG electrodes. A fundamental assumption is that the different sources are statistically mutually independent at each time n, each source characterized by its individual non-Gaussian probability density functions. This assumption involves the sources of ventricular and atrial origin as well as noise sources such as muscular activity, respiration and electrode movement. While the two cardiac activities are strongly coupled in the normal heart, they can be treated as independent processes during AF as the atrial wavefronts lead to ventricular depolarization at highly irregular times (Rieta *et al.* 2004).

Independent component (IC) analysis is a powerful technique for blind source separation whose purpose is to find a linear transformation,

$$\boldsymbol{y}(n) = \boldsymbol{B}\boldsymbol{x}(n), \tag{2.21}$$

so that the resulting components of $\boldsymbol{y}(n)$ become independent in the statistical sense, serving as estimates of the source signals $\boldsymbol{s}(n)$. Since strict statistical independence cannot be achieved in practice, $\boldsymbol{B}$ is chosen so that some suitable function designed to measure independence is maximized, usually synonymous to maximizing non-Gaussianity. The linear transformation in (2.21) is, in contrast to PCA, not constrained to be orthogonal, but can have any structure as long as $\boldsymbol{B}$ has full column rank. A description of methods for determining the ICs $\boldsymbol{y}(n)$ is outside the scope of this paper. The interested reader is referred to the literature available on this topic (e.g. Hyvärinen *et al.* 2001).

IC analysis (ICA) has been investigated for the extraction of atrial activity (Rieta *et al.* 2004; Castells *et al.* 2005*b*; Phlypo *et al.* 2007). This technique can extract atrial activity in signals as short as a few seconds; this is in contrast to ABS and variants where several beats are required to produce an average. With ICA, a component is selected as a 'global' atrial signal with contributions from all leads. The amplitude of this signal is normalized and therefore does not easily translate to clinical terms. As a result, lead-related information is lost as the ICs derive from one or several signal sources and not from a particular position on the body surface.

The assumption of *non-Gaussian source signals* is valid when it comes to ventricular activity, because histogram analysis of the amplitude of ECGs at high signal-to-noise ratios (SNRs) shows that the kurtosis is much larger than zero, i.e. the ventricular activity is clearly super-Gaussian (Rieta *et al.* 2004; Clifford *et al.* 2006). On the other hand, this assumption is less valid for atrial activity as its kurtosis may approach zero (Castells *et al.* 2005*b*), although it was initially suggested to have a sub-Gaussian distribution (Rieta *et al.* 2004). While certain types of noise are clearly super-Gaussian, e.g. powerline interference, other types such as muscular activity are approximately Gaussian (Clifford *et al.* 2006), implying that the IC with atrial activity will contain some muscular noise.

The validity of the assumption of *linear, instantaneous mixing*, described by the matrix $\boldsymbol{A}$, has been motivated by the structure of the solution to the so-called forward problem (Rieta *et al.* 2004). In that solution, the electrical potential on the body surface is obtained by adding the partial contributions of the potentials on the epicardial surface, each point being weighted by a linear, instantaneous transfer coefficient. The coefficients account for the conductivity of the human torso when approximated as an isotropic, homogeneous volume conductor. It should be noted that the validity of this assumption may be questioned because the cardiac source rotates over time due to, for example, respiration (Clifford *et al.* 2006).

A crucial step in ICA-based atrial activity extraction is to identify the IC that contains atrial activity. The first algorithm proposed for this purpose made use of kurtosis-based reordering of the components, relying on the assumption that sub-Gaussian sources are associated with atrial activity, approximately Gaussian ones with various types of noise, whereas super-Gaussian sources are associated with ventricular activity (Rieta *et al.* 2004). Figure 3 illustrates the outcome of ICA for a 12-lead ECG, the ICs being displayed in increasing order of kurtosis. The atrial activity is mostly contained in the first IC.

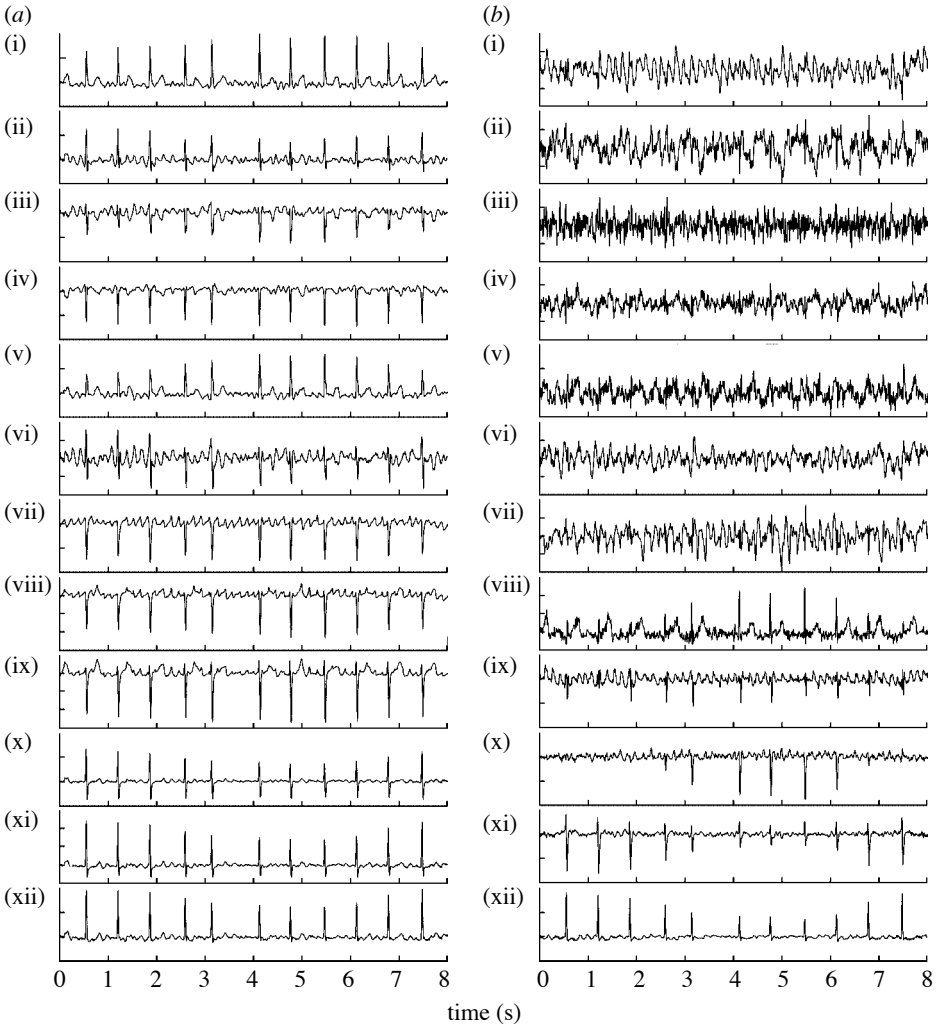

Figure 3. Atrial activity extraction using ICA. (*a*) The original 12-lead ECG (i) I, (ii) II, (iii) III, (iv) aVR, (v) aVL, (vi) aVF, (vii–xii) V1–V6 and (*b*) associated ICs, i.e. $\boldsymbol{y}(n)$ (i–xii) components 1–12. (Reprinted with permission from Rieta *et al.* (2004).)

3. AF frequency and beyond

Following atrial activity extraction, a power spectrum is usually computed, which typically exhibits a distinct peak whose location determines the most common fibrillatory rate of nearby endocardial sites (Bollmann *et al.* 1998; Holm *et al.* 1998). Most studies make use of non-parametric, Fourier-based spectral analysis in which the atrial signal is divided into shorter, overlapping segments, each segment subjected to windowing (e.g. Welch's method). The desired power spectrum is obtained by averaging the power spectra of the respective segments.

(*a*) *Time–frequency analysis*

Power spectral analysis reflects the average signal behaviour during the analysed time interval, but cannot characterize temporal variations in AF frequency. The presence of bi- or multimodal spectral peaks, reported in some early studies (Holm *et al.* 1998; Pehrson *et al.* 1998), may be interpreted as spatial variation in AF frequency. When these results are seen in the light of time–frequency analysis, such peaks can be explained by temporal variation in AF frequency rather than by spatial variation. This type of analysis is a powerful tool for unveiling temporal variations of the atrial signal, whether such variations are spontaneous or due to intervention. Similar to power spectral analysis, many methods have been developed for time–frequency analysis but few are today used for AF analysis.

A novel approach to time–frequency analysis was recently presented in which the time–frequency distribution, defined by local power spectra from successive 1 s segments, is decomposed into a spectral profile and trends describing variations in AF frequency and morphology (Stridh *et al.* 2004). The spectral profile differs from the conventional power spectrum in that the local spectra have been frequency-aligned before spectral averaging. As a result, the peaks of the spectral profile become more distinct, implying that determination of the harmonic structure of the atrial signal, i.e. the f-wave morphology, is facilitated.

In this approach, the atrial signal is first divided into overlapping segments $\boldsymbol{x}_l$, indexed by l, for which the spectrum $\boldsymbol{q}_l$ is obtained using a non-uniform Fourier transform,

$$\boldsymbol{q}_l = \boldsymbol{F}\boldsymbol{W}\boldsymbol{x}_l, \tag{3.1}$$

where the elements of the $N\times N$ diagonal matrix $\boldsymbol{W}$ define a window function. The $K\times N$ matrix $\boldsymbol{F}$ defines the K-point non-uniform transform

$$\boldsymbol{F} = [\,\mathbf{1} \quad \mathrm{e}^{-j2\pi \boldsymbol{f}} \quad \mathrm{e}^{-j2\pi \boldsymbol{f}2} \quad \ldots \quad \mathrm{e}^{-j2\pi \boldsymbol{f}(N-1)}\,], \tag{3.2}$$

where $\boldsymbol{f} = [\,f_0 \quad \ldots \quad f_{K-1}\,]^{\mathrm{T}}$ is a logarithmically scaled frequency vector, given by

$$f_k = f_0 \cdot 10^{k/K}, \quad k = 0, 1, \ldots, K-1, \tag{3.3}$$

and $\mathbf{1}$ is a column vector of length K with all elements equal to one. The logarithmic frequency scale is employed because doubling in frequency for the entire spectrum corresponds to the same number of frequency bins and, therefore, the harmonic pattern of two spectra with different fundamental frequency can be matched. This property is important when estimating the frequency shift of each $\boldsymbol{q}_l$ that best matches the spectral profile.

Each spectrum $\boldsymbol{q}_l$ is assumed to be modelled by $\boldsymbol{s}_l$ which is a frequency-shifted and amplitude-scaled version of a known spectral profile $\boldsymbol{\phi}_l$,

$$\boldsymbol{s}_l = a_l \boldsymbol{J}_{\theta_l} \boldsymbol{\phi}_l, \tag{3.4}$$

where the matrix $\boldsymbol{J}_{\theta_l}$ performs the frequency shift by selecting the appropriate interval of $\boldsymbol{\phi}_l$, cf. (2.3). The amplitude scaling parameter a_l and the frequency-shift parameter θ_l can be estimated by minimizing the quadratic cost function $J(\theta_l, a_l)$ so that the model $\boldsymbol{s}_l$ matches optimally $\boldsymbol{q}_l$,

$$J(\theta_l, a_l) = (\boldsymbol{q}_l - \boldsymbol{s}_l)^{\mathrm{T}} \boldsymbol{D} (\boldsymbol{q}_l - \boldsymbol{s}_l), \tag{3.5}$$

where $\boldsymbol{D}$ is a $K\times K$ diagonal matrix designed to weight the error of the frequency components differently, to compensate for the logarithmic frequency scaling. Minimization of (3.5) results in the following estimators of frequency-shift and amplitude scaling (Stridh *et al.* 2004):

$$\hat{\theta}_l = \arg \max_{\theta_l} \left[\boldsymbol{q}_l^{\mathrm{T}} \boldsymbol{D}^{1/2} \boldsymbol{J}_{\theta_l} \boldsymbol{D}^{1/2} \boldsymbol{\phi}_l \right], \tag{3.6}$$

$$\hat{a}_l = \boldsymbol{q}_l^{\mathrm{T}} \boldsymbol{D}^{1/2} \boldsymbol{J}_{\hat{\theta}_l} \boldsymbol{D}^{1/2} \boldsymbol{\phi}_l. \tag{3.7}$$

Since the spectral profile is not known *a priori*, a self-tuning method has been employed to estimate the spectral profile from the prevailing signal characteristics. Exponential averaging has been found useful for this purpose, defined by

$$\hat{\boldsymbol{\phi}}_{l+1} = (1-\alpha_l)\hat{\boldsymbol{\phi}}_l + \alpha_l \frac{\boldsymbol{J}_{-\hat{\theta}_l} \tilde{\boldsymbol{q}}_l}{\|\boldsymbol{J}_{-\hat{\theta}_l} \tilde{\boldsymbol{q}}_l\|}, \quad l>0, \tag{3.8}$$

where the gain α_l $(0<\alpha_l<1)$ is set to 0 when the signal is unreliable. Here, the tilde notation indicates that $\boldsymbol{q}_l$ has been pre- and appended with a sufficient number of points in order to allow for frequency shifting.

A point in the AF frequency trend is obtained by determining the peak location in the spectral profile $\hat{\boldsymbol{\phi}}_l$ and then correcting it with $\hat{\theta}_l$. The amplitude estimate $\hat{a}_l$ can be used as a measure reflecting f-wave amplitude; it can also serve as a normalization factor when evaluating the model error $J(\hat{\theta}_l, \hat{a}_l)$.

Figure 4 illustrates time–frequency analysis of AF by displaying the logarithmic short-term Fourier transform (STFT), the spectral profile $\boldsymbol{\phi}_l$ as it appears at the end of the analysed interval and the AF frequency trend. For comparison, the power spectrum for the analysed interval is included, exhibiting a much wider peak for AF frequency.

(*b*) *Robust time–frequency analysis*

A number of approaches have been suggested to make time–frequency analysis more robust to poor SNR of the atrial signal. The first approach is to make use of a signal structure feature that indicates when AF is present (Stridh *et al.* 2006). The feature exploits the fact that $\boldsymbol{\phi}_l$ must exhibit a certain harmonic structure to reflect AF. In addition, the local signal properties must fit the signal model sufficiently well as judged by the model error $(\boldsymbol{q}_l - \boldsymbol{s}_l)$.

Another approach is to use a hidden Markov model to improve noise robustness when tracking AF frequency. A sequence of observed frequency states is obtained from the residual ECG, using the STFT. Based on the observed state sequence, the Viterbi algorithm retrieves the optimal sequence by exploiting the state transition matrix, incorporating knowledge of AF characteristics, and the observation matrix, incorporating knowledge of the frequency estimation method and SNR (Sandberg *et al.* 2008).

Yet another approach is to use a spectral model that represents the fundamental frequency and harmonics with Gaussian functions, accounting for essential spectral characteristics of AF (Corino *et al.* 2007). With this approach, the update of the spectral profile in (3.8) is controlled by the error between $\boldsymbol{q}_l$ and the fitted model spectrum so that α_l is set to 0 when the error exceeds a certain threshold.

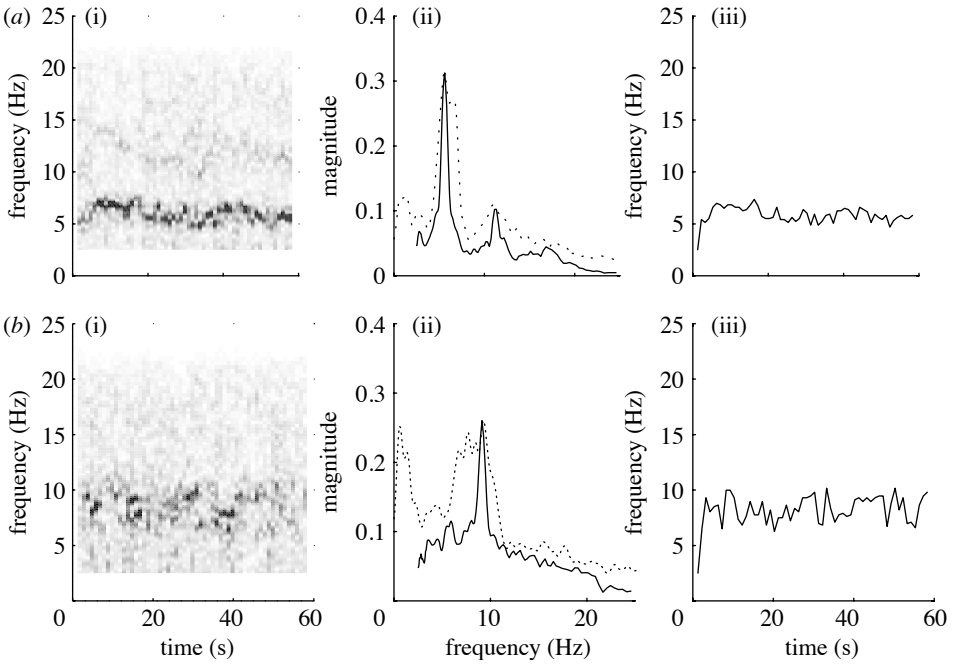

Figure 4. Analysis of 60 s signals with AF producing the STFT with (i) logarithmic frequency scale, (ii) the spectral profile (solid line) and the conventional magnitude spectrum (dotted line), and (iii) the AF frequency trend. (*a*) The spectral profile has a relatively large first harmonic and a variation in AF frequency within 5–7 Hz. (*b*) A high AF frequency coupled to a large variation (7–10 Hz).

4. Clinical applications

(*a*) *Method validation and reproducibility*

A direct comparison between endocardially recorded electrograms and body surface recordings clearly evidences the validity of fibrillatory rate obtained from the surface ECG as an index of the length of the average atrial fibrillatory cycle. While in a preliminary report median right atrial and surface ECG rates exhibited only moderate correlation (Slocum & Ropella 1994), dominant rates determined from lead V1 were in close agreement with the rates of the right atrial free wall (Bollmann *et al.* 1998; Holm *et al.* 1998) and those from an oesophageal lead reflected atrial septal and left atrial activity (Holm *et al.* 1998). Importantly, rate differences and variability between ECG and electrograms increase with growing anatomical distance (right atrium coronary sinus pulmonary veins) to lead V1. Moreover, it can be speculated that with the currently available technology, localized intra-atrial phenomena such as micro-re-entry cannot be recorded on the surface. However, since frequency gradients between right and left atrial sites are dependent on the AF type (Lazar *et al.* 2004), overall, there is also a good correlation of fibrillatory rates of left atrial sites and V1 (figure 5; Husser *et al.* 2007*b*). Nevertheless, non-standard surface ECG lead positions such as at the posterior chest wall for better characterization of left atrial/pulmonary vein activity or identification of spatial variation have been validated in a preliminary study (Petrutiu *et al.* 2006), and their feasibility for time–frequency analysis has been suggested (Husser *et al.* 2007*c*).

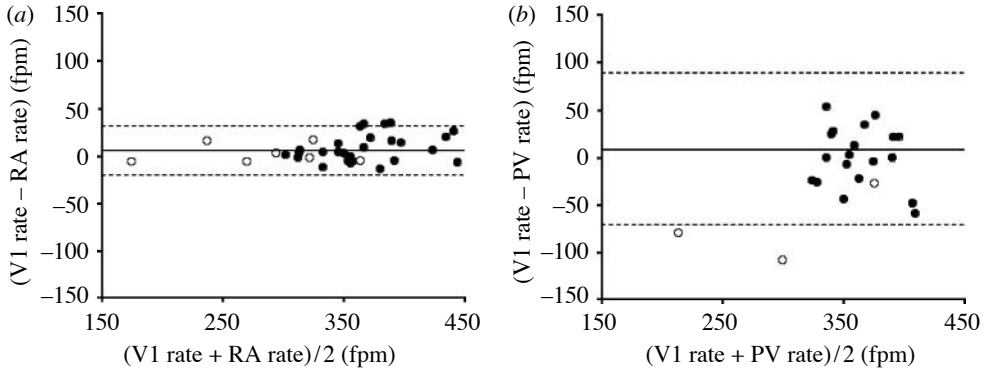

Figure 5. Agreement between fibrillatory rates simultaneously recorded from (*a*) surface ECG lead V1 and right atrium and (*b*) pulmonary vein (Bland–Altman plots). Open circles signify 'amiodarone' and filled circles 'no antiarrhythmic drug'. RA and PV denote right atrium and pulmonary vein, respectively, and fpm denotes fibrillations per minute.

In persistent AF, there is minor short-term rate variability within 30 min (Bollmann *et al.* 1998; Holm *et al.* 1998), while repeated daily measurements at identical medication at the same time under similar conditions disclose an insignificant rate variability (Meurling *et al.* 1999). Surface ECG AF wave characteristics have also been shown to be reproducible over 24 hours in clinical stable AF patients even in 10 s ECG segments as acquired in 12-lead ECGs (Xi *et al.* 2004), although longer recordings may increase reproducibility (Holm *et al.* 1998).

(*b*) *Exploration of AF pathophysiology*

Atrial fibrillatory rate has been used to quantify AF-associated changes of atrial electrophysiology, so-called electrical remodelling, and to study the effects of changes in autonomic tone (Allessie *et al.* 2002). For instance, long-term monitoring of up to 14 months revealed a progression of atrial remodelling quantified by a rate increase in patients with persistent AF (Sasaki *et al.* 2006). Similarly, fibrillatory rate increased over a period of 12 months in patients with paroxysmal AF, which was associated with a prolongation of AF episodes. Interestingly, verapamil treatment in a subgroup of patients prevented this unfavourable effect (Niwano *et al.* 2007).

The natural course of fibrillatory rate in single paroxysmal AF episodes has been studied. Typical findings were a rate increase at the onset of an episode (Bollmann *et al.* 1999) and a rate decrease prior to termination (Bollmann *et al.* 1999; Fujiki *et al.* 2003*a*). In more detail, long AF episodes showed a gradual rate increase over the first 4 min, while short episodes showed an increase only from the first to the second minute (Petrutiu *et al.* 2007*b*). Conversely, spontaneous AF termination was associated with a rate decrease that occurred, however, within second(s) before termination (Petrutiu *et al.* 2007*a*).

The circadian rate variability in persistent AF has also been explored. Fibrillatory rate obtained from Holter ECGs showed a significant decrease at night and an increase in the morning hours. In 6 out of 30 subjects studied by our group (Bollmann *et al.* 2000), dominant nocturnal fibrillatory rate increased, however, concomitantly with a decrease in ventricular rate, while the opposite

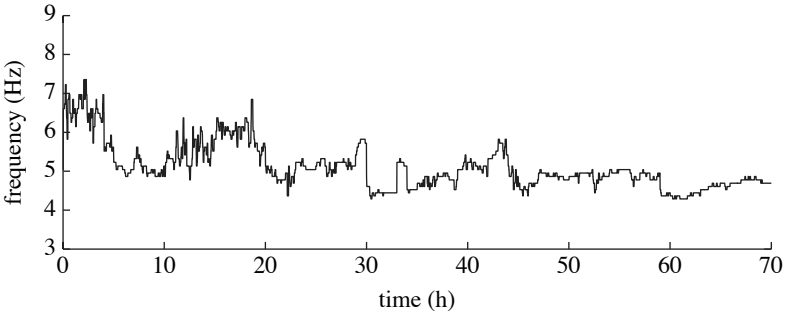

Figure 6. Atrial fibrillatory rate response to an antiarrhythmic drug (flecainide). The drug was given at the onset of the recording and after 16, 27, 42, 52 and 66 hours.

change occurred in the morning hours. These findings point to individual modulatory effects of the autonomic nervous system. This observation is even further supported by several studies in which autonomic manoeuvres have been applied such as vagal or sympathetic stimulation during experimental conditions.

With the availability of instantaneous fibrillatory rates from time–frequency analysis, their second-to-second variation can be explored. Using this approach, controlled respiration caused cyclic fluctuations in fibrillatory rate in patients with long-duration AF, which was related to parasympathetic modulation of the atrial refractory period (Stridh *et al.* 2003; Holmqvist *et al.* 2005). Finally, the relationship between genotype and ECG phenotype is currently being explored by our group. In a preliminary study (Bollmann *et al.* 2007), we were the first to demonstrate that rate is at least in part determined by KCNE1 (S38G) genotype, suggesting this potassium channel gene variant exerts functional effects on atrial electrophysiology.

(*c*) *Clinical AF management*

In the clinical setting, fibrillatory rate has been used to predict the spontaneous behaviour, to monitor interventions such as antiarrhythmic drug administration (figure 6), or AF ablation, and to predict the response to various therapies. Fibrillatory rate has been shown to be highly predictive of spontaneous termination of paroxysmal AF. In a study of 30 ECG recordings, a low fibrillatory rate was able to identify patients with spontaneously terminating AF with a high accuracy (Nilsson *et al.* 2006). Similarly, in new-onset AF, sensitivity and specificity for predicting AF termination were strongly related to fibrillatory rate. Sensitivity and specificity were 89 and 71 per cent for a fibrillatory rate of 355 fibrillations per minute (fpm; Husser *et al.* 2007*a*).

Fibrillatory rate changes in response to linear left atrial ablation have also been monitored non-invasively and the effect on fibrillatory rate of roof and mitral isthmus lines quantified (Raine *et al.* 2005). Even though there was a trend to lower baseline rates with successful ablation, this study was not powered to predict outcome, although an invasive study supports this conclusion (Haissaguerre *et al.* 2004).

Interestingly, it is also possible to identify suitable candidates for pharmacological cardioversion. A baseline fibrillatory rate of 360 fpm or lower was highly sensitive and specific for prediction of AF termination following

intravenous ibutilide or oral flecainide (Bollmann *et al.* 1998). By contrast, no baseline fibrillatory rate difference between patients who converted to sinus rhythm and those who did not following oral bepridil administration has been noted. Instead, larger rate increases were associated with AF termination (Fujiki *et al.* 2003*b*).

Previous investigations have shown that most AF relapses occur within the first weeks after cardioversion with decreased but constant recurrence rates thereafter (Tieleman *et al.* 1998). Early vulnerability to AF re-initiation within this time period is related to electrophysiological abnormalities, while structural abnormalities seem to be primarily responsible for later AF recurrences (Everett *et al.* 2000). Consequently, characterization of atrial electrophysiology has been suggested for identification of patients at risk for early AF recurrence (Bollmann 2000).

Higher rates have been reported in relapsed patients immediately prior to internal (Bollmann *et al.* 2002) or external cardioversion (Bollmann *et al.* 2003; Holmqvist *et al.* 2006) when compared with non-relapsed patients. So far, one study has investigated the combined predictive value of fibrillatory rate and echocardiographic left atrial parameters for predicting AF recidivism (Bollmann *et al.* 2003). It could be demonstrated that the combination of fibrillatory rate and systolic left atrial area predicted early AF recurrence after successful cardioversion with high accuracy and was able to provide individual risk estimates. It needs to be pointed out, however, that all patients in this study received class I or III antiarrhythmic drugs. Of note, in patients of a more recent investigation who received no additional antiarrhythmic drugs (Holmqvist *et al.* 2006), the most prominent predictive effect of fibrillatory rate was found only in those with a short AF duration (less than 30 days).

5. Conclusions

Recent advances in signal processing have made it possible to separate atrial activity from ventricular activity in the ECG. With the availability of an atrial signal comes the challenge to develop approaches that explore the information of the fibrillatory waves, and time–frequency analysis is one useful approach. Such information will provide better explanations of the electrophysiological phenomena as well as improving diagnosis and treatment. Improved selection of candidates for cardioversion and other interventional procedures is one important goal with the development of such methods.

This work was supported in part by the Swedish Research Council, Volkswagen Foundation, Germany, and the NordForsk network ‘Electrocardiology in Atrial Fibrillation’.

References

Allessie, M., Ausma, J. & Schotten, U. 2002 Electrical, contractile and structural remodeling during atrial fibrillation. *Cardiovasc. Res.* **54**, 230–246. (doi:10.1016/S0008-6363(02)00258-4)

Bollmann, A. 2000 Quantification of electrical remodeling in human atrial fibrillation. *Cardiovasc. Res.* **47**, 207–209. (doi:10.1016/S0008-6363(00)00133-4)

Bollmann, A., Kanuru, N., McTeague, K., Walter, P., DeLurgio, D. B. & Langberg, J. 1998 Frequency analysis of human atrial fibrillation using the surface electrocardiogram and its response to ibutilide. *Am. J. Cardiol.* **81**, 1439–1445. (doi:10.1016/S0002-9149(98)00210-0)

Bollmann, A., Sonne, K., Esperer, H. D., Toepffer, I., Langberg, J. J. & Klein, H. U. 1999 Non-invasive assessment of fibrillatory activity in patients with paroxysmal and persistent atrial fibrillation using the Holter ECG. *Cardiovasc. Res.* **44**, 60–66. (doi:10.1016/S0008-6363(99)00156-X)

Bollmann, A., Sonne, K., Esperer, H., Toepffer, I. & Klein, H. 2000 Circadian variations in atrial fibrillatory frequency in persistent human atrial fibrillation. *Pacing Clin. Electrophysiol.* **23**, 1867–1871.

Bollmann, A., Mende, M., Neugebauer, A. & Pfeiffer, D. 2002 Atrial fibrillatory frequency predicts atrial defibrillation threshold and early arrhythmia recurrence in patients undergoing internal cardioversion of persistent atrial fibrillation. *Pacing Clin. Electrophysiol.* **25**, 1179–1184. (doi:10.1046/j.1460-9592.2002.01179.x)

Bollmann, A. *et al.* 2003 Echo- and electrocardiographic predictors for atrial fibrillation recurrence following cardioversion. *J. Cardiovasc. Electrophysiol.* **14**, 162–165. (doi:10.1046/j.1540.8167.90306.x)

Bollmann, A. *et al.* 2006 Analysis of surface electrocardiograms in a trial fibrillation: techniques, research, and clinical applications. *Europace* **8**, 911–926. (doi:10.1093/europace/eul113)

Bollmann, A., Husser, D., Stridh, M., Sörnmo, L., Hindricks, G., Roden, D. M. & Darbar, D. 2007 A genotype dependent intermediate ECG phenotype in patients with persistent lone atrial fibrillation (abstract). *Circulation* **116**, 477.

Castells, F., Mora, C., Rieta, J. J., Moratal-Pérez, D. & Millet, J. 2005*a* Estimation of atrial fibrillatory wave from single-lead atrial fibrillation electrocardiograms using principal component analysis concepts. *Med. Biol. Eng. Comput.* **43**, 557–560. (doi:10.1007/BF02351028)

Castells, F., Rieta, J. J., Millet, J. & Zarzoso, V. 2005*b* Spatiotemporal blind source separation approach to atrial activity estimation in atrial tachyarrhythmias. *IEEE Trans. Biomed. Eng.* **52**, 258–267. (doi:10.1109/TBME.2004.840473)

Castells, F., Laguna, P., Sörnmo, L., Bollmann, A. & Millet, J. 2007 Principal component analysis in ECG signal processing. *J. Adv. Signal Proc.* **2007**, 21. (doi:10.1155/2007/74580)

Clifford, G. D., Azuaje, F. & McSharry, P. E. (eds) 2006 *Advanced methods and tools for ECG data analysis*. Boston, MA: Artech House.

Corino, V., Mainardi, L., Bollmann, A., Husser, D., Stridh, M. & Sörmno, L. 2007 A Gaussian mixture model for time–frequency analysis during atrial fibrillation. In *Proc. IEEE Conf. of Engineering in Medicine and Biology.*

Everett IV, T. H., Li, H., Mangrum, J. M., McRury, I. D., Mitchell, M. A., Redick, J. A. & Haines, D. E. 2000 Electrical, morphological, and ultrastructural remodeling and reverse remodeling in a canine model of chronic atrial fibrillation. *Circulation* **102**, 1454–1460.

Fujiki, A., Sakabe, M., Nishida, K., Mizumaki, K. & Inoue, H. 2003*a* Role of fibrillation cycle length in spontaneous and drug-induced termination of human atrial fibrillation—spectral analysis of fibrillation waves from surface electrocardiogram. *Circ. J.* **67**, 391–395. (doi:10.1253/circj.67.391)

Fujiki, A., Tsuneda, T., Sugao, M., Mizumaki, K. & Inoue, H. 2003*b* Usefulness and safety of bepridil in converting persistent atrial fibrillation to sinus rhythm. *Am. J. Cardiol.* **92**, 472–475. (doi:10.1016/S0002-9149(03)00672-6)

Haissaguerre, M. *et al.* 2004 Changes in atrial fibrillation cycle length and inducibility during catheter ablation and their relation to outcome. *Circulation* **109**, 3007–3013. (doi:10.1161/01.CIR.0000130645.95357.97)

Holm, M. *et al.* 1998 Non-invasive assessment of atrial refractoriness during atrial fibrillation in man—introducing, validating, and illustrating a new ECG method. *Cardiovasc. Res.* **38**, 69–81. (doi:10.1016/S0008-6363(97)00289-7)

Holmqvist, F., Stridh, M., Waktare, J. E. P., Brandt, J., Sörnmo, L., Roijer, A., Olsson, S. B. & Meurling, C. J. 2005 Rapid fluctuations in atrial fibrillatory electrophysiology detected during controlled respiration. *Am. J. Physiol.* (*Heart Circ. Physiol.*) **289**, H754–H760. (doi:10.1152/ajpheart.00075.2005)

Holmqvist, F., Stridh, M., Waktare, J. E., Sörnmo, L., Olsson, S. B. & Meurling, C. J. 2006 Atrial fibrillatory rate and sinus rhythm maintenance in patients undergoing cardioversion of persistent atrial fibrillation. *Eur. Heart J.* **27**, 2201–2207. (doi:10.1093/eurheartj/ehl098)

Husser, D., Cannom, D. S., Bhandari, A. K., Stridh, M., Sörnmo, L., Olsson, S. B. & Bollmann, A. 2007*a* Electrocardiographic characteristics of fibrillatory waves in new-onset atrial fibrillation. *Europace* **9**, 638–642. (doi:10.1093/europace/eum074)

Husser, D., Stridh, M., Cannom, D. S., Bhandari, A. K., Girsky, M. J., Kang, S., Sörnmo, L., Olsson, S. B. & Bollmann, A. 2007*b* Validation and clinical application of time–frequency analysis of atrial fibrillation electrocardiograms. *J. Cardiovasc. Electrophysiol.* **18**, 41–46. (doi:10.1111/j.1540-8167.2006.00683.x)

Husser, D., Stridh, M., Sörnmo, L., Toepffer, I., Klein, H. U., Olsson, S. B. & Bollmann, A. 2007*c* Electroatriography—time–frequency analysis of atrial fibrillation from modified 12-lead ECG configurations for improved diagnosis and therapy. *Med. Hypotheses* **68**, 568–573. (doi:10.1016/j.mehy.2006.08.014)

Hyvärinen, A., Karhunen, J. & Oja, E. 2001 *Independent component analysis*. New York, NY: Wiley Interscience.

Joliffe, I. T. 2002 *Principal component analysis*. Berlin, Germany: Springer.

Langley, P., Bourke, J. P. & Murray, A. 2000 Frequency analysis of atrial fibrillation. In *Proc. Computers in Cardiology*, vol. 27, pp. 65–68. Chicago, IL: IEEE Press.

Lazar, S., Dixit, S., Marchlinski, F. E., Callans, D. J. & Gerstenfeld, E. P. 2004 Presence of left-to-right atrial frequency gradient in paroxysmal but not persistent atrial fibrillation in humans. *Circulation* **110**, 3181–3186. (doi:10.1161/01.CIR.0000147279.91094.5E)

Lemay, M., Vesin, J.-M., van Oosterom, A., Jacquemet, V. & Kappenberger, L. 2007 Cancellation of ventricular activity in the ECG: evaluation of novel and existing methods. *IEEE Trans. Biomed. Eng.* **54**, 542–546. (doi:10.1109/TBME.2006.888835)

Mainardi, L., Sörnmo, L. & Cerutti, S. (eds) 2008 *Understanding atrial fibrillation: the signal processing contribution*. San Francisco, CA: Morgan & Claypool.

Meurling, C. J., Ingemansson, M. P., Roijer, A., Carlson, J., Lindholm, C. J., Smideberg, B., Sörnmo, L., Stridh, M. & Olsson, S. B. 1999 Attenuation of electrical remodelling in chronic atrial fibrillation following oral treatment with verapamil. *Europace* **1**, 234–241.

Nilsson, F., Stridh, M., Bollmann, A. & Sörnmo, L. 2006 Predicting spontaneous termination of atrial fibrillation using the surface ECG. *Med. Eng. Phys.* **26**, 802–808. (doi:10.1016/j.medengphy.2005.11.010)

Niwano, S., Fukaya, H., Sasaki, T., Hatakeyama, Y., Fujiki, A. & Izumi, T. 2007 Effect of oral L-type calcium channel blocker on repetitive paroxysmal atrial fibrillation: spectral analysis of fibrillation waves in the Holter monitoring. *Europace* **9**, 1209–1215. (doi:10.1093/europace/eum199)

Pehrson, S., Holm, M., Meurling, C., Ingemansson, M., Smideberg, B., Sörnmo, L. & Olsson, S. 1998 Non-invasive assessment of magnitude and dispersion of atrial cycle length during chronic atrial fibrillation in man. *Eur. Heart J.* **19**, 1836–1844. (doi:10.1053/euhj.1998.1200)

Petrutiu, S., Sahakian, A. V., Fisher, W. B. & Swiryn, S. 2006 Manifestation of left atrial events in the surface electrocardiogram. In *Proc. Computers in Cardiology*, vol. 33, pp. 1–4. See http://cinc.mit.edu.

Petrutiu, S., Sahakian, A. V. & Swiryn, S. 2007*a* Abrupt changes in fibrillatory wave characteristics at the termination of paroxysmal atrial fibrillation in humans. *Europace* **9**, 466–470. (doi:10.1093/europace/eum096)

Petrutiu, S., Sahakian, A. V. & Swiryn, S. 2007*b* Short-term dynamics in fibrillatory wave characteristics at the onset of paroxysmal atrial fibrillation in humans. *J. Electrocardiol.* **40**, 155–160. (doi:10.1016/j.jelectrocard.2006.10.003)

Phlypo, R., D'Asseler, Y., Lemahieu, I. & Zarzoso, V. 2007 Extraction of the atrial activity from the ECG based on independent component analysis with prior knowledge of the source kurtosis signs. In *Proc. IEEE EMBS*, pp. 6499–6502.

Raine, D., Langley, P., Murray, A., Dunuwille, A. & Bourke, J. P. 2004 Surface atrial frequency analysis in patients with atrial fibrillation: a tool for evaluating the effects of intervention. *J. Cardiovasc. Electrophysiol.* **15**, 1021–1026. (doi:10.1046/j.1540-8167.2004.04032.x)

Raine, D., Langley, P., Murray, A., Furniss, S. S. & Bourke, J. P. 2005 Surface atrial frequency analysis in patients with atrial fibrillation: assessing the effects of linear left atrial ablation. *J. Cardiovasc. Electrophysiol.* **16**, 838–844. (doi:10.1111/j.1540-8167.2005.40456.x)

Rieta, J. J., Castells, F., Sánchez, C., Zarzoso, V. & Millet, J. 2004 Atrial activity extraction for atrial fibrillation analysis using blind source separation. *IEEE Trans. Biomed. Eng.* **51**, 1176–1186. (doi:10.1109/TBME.2004.827272)

Sandberg, F., Stridh, M. & Sörnmo, L. 2008 Robust time–frequency analysis of atrial fibrillation using hidden Markov models. *IEEE Trans. Biomed. Eng.* **55**, 502–511. (doi:10.1109/TBME.2007.905488)

Sasaki, T. *et al.* 2006 Long-term follow-up of changes in fibrillation waves in patients with persistent atrial fibrillation: spectral analysis of surface ECG. *Circ. J.* **70**, 169–173. (doi:10.1253/circj.70.169)

Slocum, J. E. & Ropella, K. M. 1994 Correspondence between the frequency domain characteristics of simultaneous surface and intra-atrial recordings of atrial fibrillation. In *Proc. Computers in Cardiology*, vol. 21, pp. 781–784.

Slocum, J., Byrom, E., McCarthy, L., Sahakian, A. V. & Swiryn, S. 1985 Computer detection of atrioventricular dissociation from surface electrocardiograms during wide QRS complex tachycardia. *Circulation* **72**, 1028–1036.

Slocum, J., Sahakian, A. V. & Swiryn, S. 1992 Diagnosis of atrial fibrillation from surface electrocardiograms based on computer-detected atrial activity. *J. Electrocardiol.* **25**, 1–8. (doi:10.1016/0022-0736(92)90123-H)

Stridh, M. & Sörnmo, L. 2001 Spatiotemporal QRST cancellation techniques for analysis of atrial fibrillation. *IEEE Trans. Biomed. Eng.* **48**, 105–111. (doi:10.1109/10.900266)

Stridh, M., Sörnmo, L., Meurling, C. J. & Olsson, S. B. 2003 Detection of autonomic modulation in permanent atrial fibrillation. *Med. Biol. Eng. Comput.* **41**, 625–629. (doi:10.1007/BF02349969)

Stridh, M., Sörnmo, L., Meurling, C. J. & Olsson, S. B. 2004 Sequential characterization of atrial tachyarrhythmias based on ECG time–frequency analysis. *IEEE Trans. Biomed. Eng.* **51**, 100–114. (doi:10.1109/TBME.2003.820331)

Stridh, M., Bollmann, A., Olsson, S. B. & Sörnmo, L. 2006 Time–frequency analysis of atrial tachyarrhythmias: detection and feature extraction. *IEEE Eng. Med. Biol. Mag.* **25**, 31–39. (doi:10.1109/EMB-M.2006.250506)

Tieleman, R. G., van Gelder, I. C., Crijns, H. J., de Kam, P. J., van den Berg, M. P., Haaksma, J., van der Woude, J. J. & Allessie, M. A. 1998 Early recurrences of atrial fibrillation after electrical cardioversion: a result of fibrillation-induced electrical remodeling of the atria? *J. Am. Coll. Cardiol.* **31**, 167–173. (doi:10.1016/S0735-1097(97)00455-5)

van Oosterom, A. 2003 The dominant T wave and its significance. *J. Cardiovasc. Electrophysiol.* **14**, S180–S187. (doi:10.1046/j.1540.8167.90309.x)

Waktare, J., Hnatkova, K., Meurling, C. J., Nagayoshi, H., Janota, T., Camm, A. J. & Malik, M. 1998 Optimal lead configuration in the detection and subtraction of QRS and T wave templates in atrial fibrillation. In *Proc. Computers in Cardiology*, pp. 629–632. Chicago, IL: IEEE Press.

Xi, Q., Sahakian, A. V., Ng, J. & Swiryn, S. 2004 Atrial fibrillatory wave characteristics on surface electrocardiogram. *J. Cardiovasc. Electrophysiol.* **15**, 911–917.